

Development and demonstration of a multi-channel spheroidal focusing device for neutron beams

H Hayashida¹, K Soyama¹, D Yamazaki¹, R Maruyama¹ and K Yamamura²

¹ J-PARC Center, Japan Atomic Energy Agency, Tokai, Ibaraki 319-1195, Japan

² Department of Precision Science & Technology, Osaka University, Suita, Osaka 565-0871, Japan

E-mail: hayashida.hirotooshi@jaea.go.jp

Abstract. A multi-channel neutron focusing mirror is a compact device that can effectively enhance neutron intensity because the multi-channel structure can cover a large divergence of a neutron beam. In this study, we attempted to develop a compact multi-channel spheroidal (MS) neutron focusing device for two-dimensional focusing. A prototype of the MS mirror consists of three spheroidal mirrors of different diameters. The mirrors are fabricated through the copper plating method without supermirror coating and are aligned coaxially using ring-shaped spacers. The MS mirror was demonstrated at beam line 10 NOBORU port at J-PARC, which provides neutron beams with time-of-flight spectra. A gain factor of 6 in neutron intensity was obtained over wavelengths greater than 0.5 nm, and an imaging test with sample scanning could be performed with an exposure time of 10 s. A Gd-patterned standard sample was employed and a 2D image with a spatial resolution of 200 μm was successfully obtained.

1. Introduction

Focusing devices are often used to increase neutron intensity over a minute area, such as a scattering experiment with small samples. Mirrors are the most commonly used focusing devices, and several types have been developed [1-4]. In this study, we attempted to develop a multi-channel neutron focusing mirror that can cover a wide divergence of neutron beams while boasting of a small size. This can be applied to a Wolter mirror, which is already very widely used in microscopy as well as in telescopes. Our approach could also lead to the realization of a compact neutron microscope, which is expected to drastically improve the spatial resolution of the neutron imaging technique. Such a microscope would have sufficient spatial resolution to be a powerful tool in magnetic imaging methods, which have been gaining prominence in recent years [5-7], to visualize magnetic domain structures of the order of micrometers. Neutron spin flippers and neutron spin analyzer are necessary components in these magnetic imaging methods. Consequently, the distance between the sample and detector is at least 500 mm. Even with a detector having a high spatial resolution of the order of micrometer, information on magnetic structure would be lost in such a long flight-path because of the divergence of the neutron beam. On the other hand, a neutron beam with large divergence can be used in the experimental setup comprising such a microscope. Because these magnetic imaging techniques consist of many parts such as a neutron spin flipper, polarizing devices, permalloy magnetic shields, and a guide field coil, sufficient space is not available for installing the microscope. Therefore a compact size is more effective for the microscope. As a first step to overcome these issues, in this study, we attempted to develop a multi-channel spheroidal (MS) mirror for focusing neutron beams.



The MS mirror was demonstrated at beam line 10 (BL10) NOBORU port at J-PARC, and an imaging test with sample scanning was performed using a focused neutron beam. The design of a prototype MS mirror is described in section 2, and a demonstration of the MS mirror is described in section 3 along with the results.

2. Design of the prototype MS mirror

Figure 1 shows a conceptual 2D diagram of the prototype MS mirror. Two focal points f_1 and f_2 are shown, and three ellipses, which represent the full spheroids of the spheroidal mirrors, are indicated with dashed lines. Thick lines along the ellipses indicate the MS mirror, and the prototype MS mirror consists of three spheroidal mirrors of different diameters. The distance between f_1 and f_2 is 1200 mm and the prototype MS mirror is designed to be placed 900 mm downstream of f_1 (300 mm upstream of f_2). The length of the MS mirror is 200 mm, and the diameters on the upstream edge of the three spheroidal mirrors (from inside to outside) are 6 mm, 8 mm and 10 mm. The incident angles of the neutron beam to the three spheroidal mirrors are also shown in Fig. 1. The three spheroidal mirrors are indicated as No. 1, No. 2, and No. 3 (from inside to outside). Incident angles as the upstream and downstream sides of mirror No. 1 are denoted by θ_{1u} and θ_{1d} , respectively. Similarly, θ_{2u} and θ_{2d} indicate those on mirror No. 2, while θ_{3u} and θ_{3d} indicate those on mirror No. 3. The neutron wavelengths reflected by the spheroidal mirrors can be estimated from these incident angles as it is known that copper has 70% the scattering length density of nickel. Table 1 lists the incident angles and neutron wavelengths corresponding to the critical angle for total reflection. The upstream and downstream sides on mirror No. 1 reflect neutron beams with wavelengths greater than 0.46 nm and 0.58 nm, respectively. Therefore, neutron beams with wavelengths greater than 0.58 nm can be reflected off the whole surface of mirror No. 1. In the case of mirrors No. 2 and No. 3, neutron beams with wavelengths greater than 0.77 nm and 0.97 nm, respectively, can be reflected off the whole surface. Although neutron beams with wavelengths shorter than 0.97 nm can be focused by coating the surface of the spheroidal mirrors with a supermirror, such a coating has not been performed in this study.

Figure 2 shows a schematic diagram of the coaxial alignment of the three spheroidal mirrors and an image of the MS mirror. The spheroidal mirrors are fabricated through the copper plating method and are aligned coaxially using ring-shaped spacers formed by winding a kapton film of width 1 mm. The surface figure error is approximately 100 nm, which is determined by the metal mold.

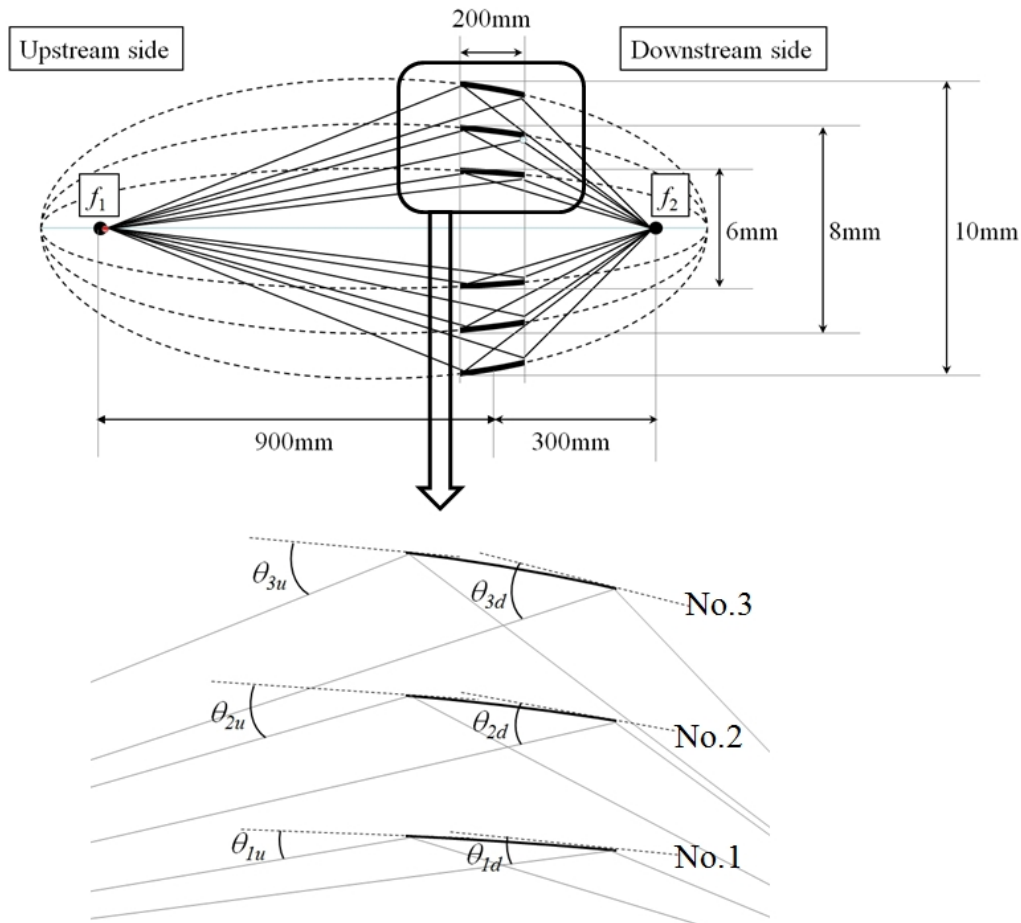


Figure 1. Conceptual 2D diagram of the prototype MS mirror. Schematics of the incident angles are enlarged.

Table 1. Incident angles at the upstream and downstream edges of each spheroidal mirror, along with neutron wavelengths corresponding to the critical angle for total reflection.

Mirror number	θ_u / degree	λ_u / nm	θ_d / degree	λ_d / nm
No.1	0.32	$0.46 \leq \lambda$	0.41	$0.58 \leq \lambda$
No.2	0.43	$0.61 \leq \lambda$	0.54	$0.77 \leq \lambda$
No.3	0.54	$0.77 \leq \lambda$	0.68	$0.97 \leq \lambda$

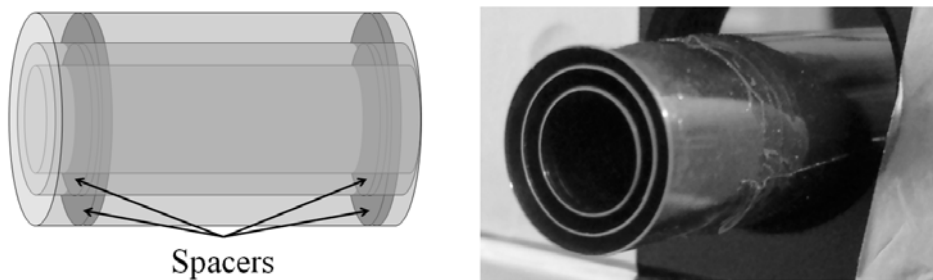


Figure 2. Schematic of the coaxial alignment of the three spheroidal mirrors and an image of the MS mirror. The ring-shaped spacers are used for coaxial alignment.

3. Demonstration and results of the prototype MS mirror

The prototype MS mirror was demonstrated at BL10 NOBORU at J-PARC. Figures 3 (a), (b), and (c) show an image of the experimental setup, and schematic diagrams of this experiment without and with the MS mirror, respectively. A pinhole slit of diameter $100\ \mu\text{m}$ is set at the focal point. The MS mirror is set upstream of the pinhole slit. The distance between the center of the MS mirror and the pinhole slit is $300\ \text{mm}$ as shown in Fig. 3(c). The MS mirror can be moved in the horizontal direction, which enables us to switch between the experimental setups with and without the MS mirror. A two-dimensional position sensitive detector (2D detector) is set downstream of the pinhole slit. The distance between the pinhole slit and the surface of the 2D detector is $130\ \text{mm}$ as shown in Fig. 3(b). A supermirror with $m = 4$ is set upstream of the MS mirror to shield the 2D detector from a direct high-energy beam. The performance of the MS mirror was evaluated using both experimental setups.

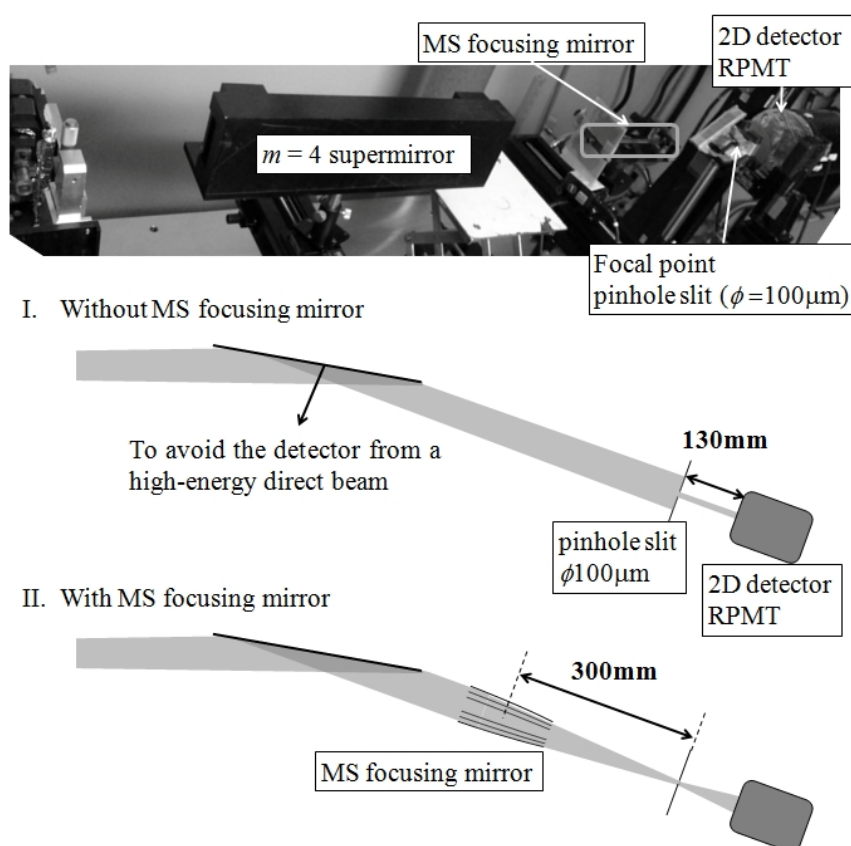


Figure 3. (a) Image of the experimental setup, (b) schematic diagram of the experiment without the MS mirror, and (c) schematic diagram of the experiment with the MS mirror.

Figure 4 shows a 2D image of the neutron beam focused by the MS mirror. A focused neutron beam has a large divergence as compared to that of its unfocused counterpart. Hence, after passing through the pinhole slit, the focused beam spreads into a ring shape at the detector position. The center spot in Fig. 4 shows a direct beam not focused by the MS mirror, and the ring shape around the center spot indicates a neutron beam focused by the MS mirror. Figure 5 shows the time-of-flight (TOF) spectra of the neutron intensity with and without the MS mirror and the ratio of these spectra. The ratio indicates a gain in neutron intensity caused by the MS mirror.

The prototype MS mirror has not been coated with supermirror and mirror No. 3 can reflect neutron beams with wavelengths greater than $0.97\ \text{nm}$, as indicated in Table 1. Mirror No. 3 does not work in this experiment, because the neutron wavelength in the BL10 NOBORU can be used up to $1\ \text{nm}$. Mirrors No. 2 and No. 1 work on neutron beams of wavelengths greater than $0.77\ \text{nm}$ and $0.58\ \text{nm}$,

respectively, as indicated in Table 1. In the wavelengths of 0.77 nm, mirrors No. 1 and No. 2 work, and the neutron intensity exhibits a gain by a factor of 7.6, which is estimated from the ratio of beam divergences between the two experimental setups. For wavelengths of 0.58 nm, only mirror No. 1 works, and the gain factor can be evaluated as 3.7. However, the gain factors between the two experimental setups for neutron wavelengths from 0.58 nm to 0.77 nm are approximately 6, as shown in Fig. 5, which is inconsistent with geometric estimations. These inconsistent results could be attributed to both setting and coaxial alignment errors. Figure 6 shows a conceptual diagram of misalignment occurring in two typical situations with a spheroidal focusing mirror. The incident angle of the neutron beam on a part of the mirror is less than the designed incident angle, and in the other part of the mirror, it is greater than the designed incident angle. In the former case, neutron beams with wavelengths shorter than the design specification can get focused by the spheroidal mirror surface, whereas in the latter, neutron wavelengths corresponding to the critical angle shift to longer wavelengths. Because of these possibilities, neutron beams with wavelengths different from the design specifications get focused. Hence, the image of the focused neutron beam on the 2D detector does not have a perfect ring shape, as shown in Fig. 4. Therefore, it can be considered that the alignment precision of the setting error and coaxial alignment error lead to results inconsistent with what is expected on the basis of design specifications.

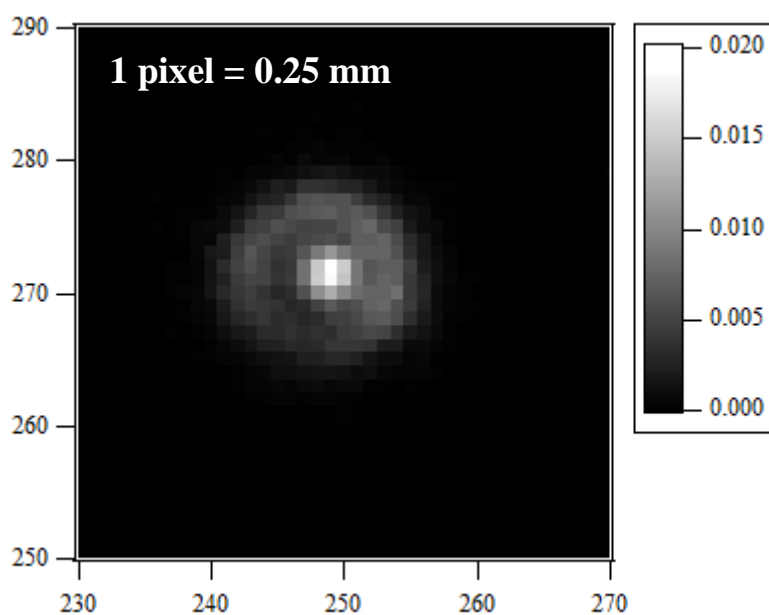


Figure 4. A 2D image of the neutron beam focused by the MS mirror. The spot at the center is the direct beam not focused by the MS mirror. The ring shape around the center spot is the beam focused by the MS mirror.

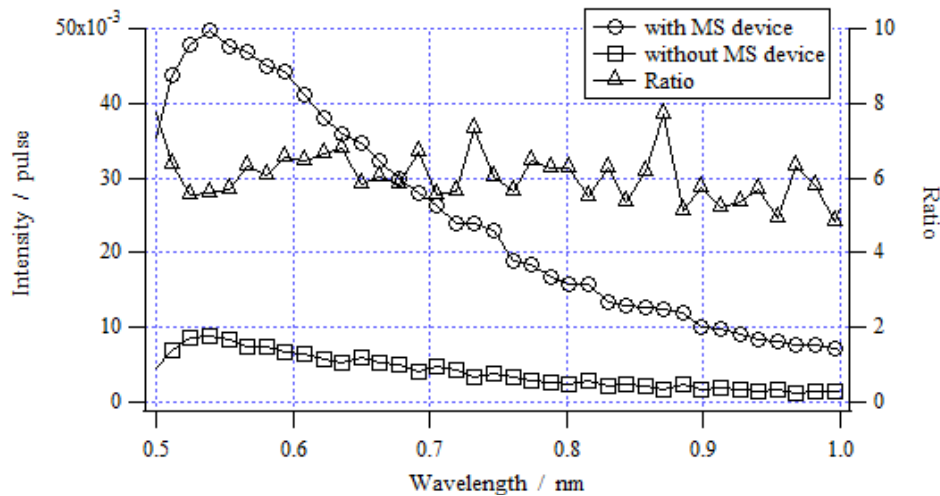


Figure 5. The circles line and the squares line show the TOF spectra with and without the MS mirror, respectively. The triangles represents the ratio of these spectra.

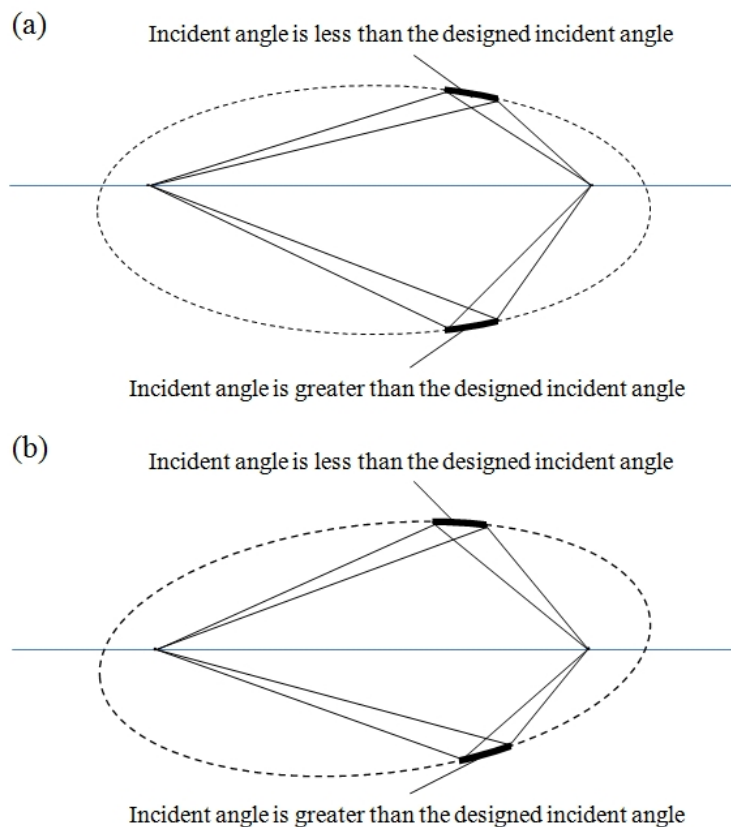


Figure 6. Conceptual diagram of two typical misalignment patterns with a spheroidal focusing mirror.

Although numerous issues remain in the MS mirror, the intensity gain factor of 6, shown in Fig. 5, and the results of the scanning imaging test are promising. Figure 7 shows a schematic of the imaging test, a picture of a test sample, and the resulting 2D image. A Gd-patterned sample, which is a standard sample made by PSI group [8], was used to evaluate spatial resolution. The pitches of the Gd patterns are 500 μm , 400 μm , 300 μm , and 200 μm (from outside), as shown in the central image in Fig. 7. The

sample was placed just downstream of the pinhole slit. A scanning pitch of the sample was $100\ \mu\text{m}$, identical to the pinhole slit size, which corresponds to neutron imaging using a 2D detector with spatial resolution of $100\ \mu\text{m}$. A 2D image obtained from scanning the sample is shown on the right in fig. 7. The scale bar of the 2D image shows integrated neutron intensity. Gd patterns with a resolution of $200\ \mu\text{m}$ can be visualized. Measurement time of each period was 10 s. The MS mirror enables us to perform the imaging test with a spatial resolution of $200\ \mu\text{m}$ within such a short measurement time.

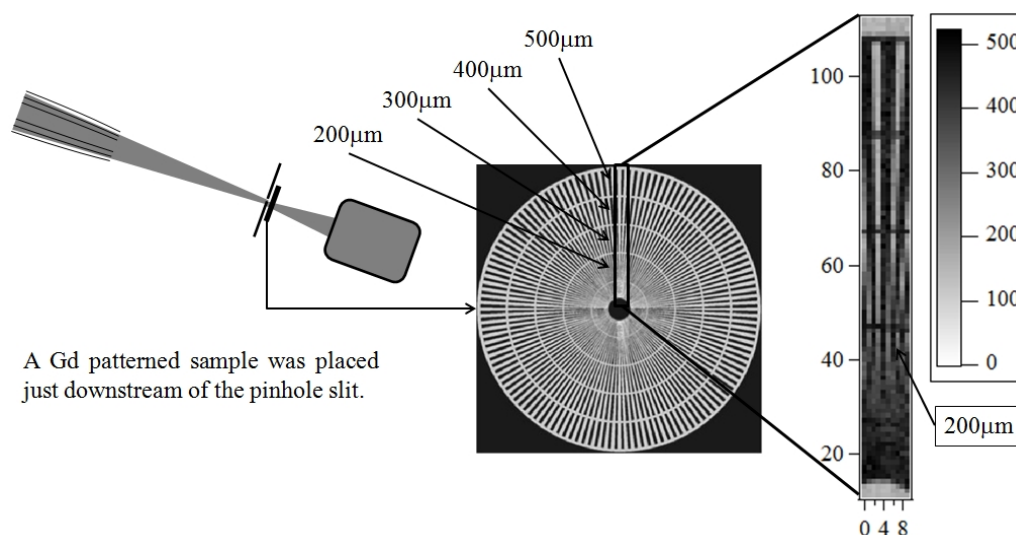


Figure 7. Schematic diagram of the imaging test, a picture of a test sample, and the resulting 2D image. A Gd patterned sample was used as a test sample.

4. Summary

A prototype MS mirror has been developed, and its demonstration for a neutron beam has been performed. The prototype MS mirror consists of three spheroidal mirrors of different diameters fabricated through the copper plating method and aligned coaxially using ring-shaped spacers. Supermirror coating was not performed on the surface of the MS mirror. The length of the MS mirror was 200 mm. The MS mirror was demonstrated at BL10 NOBORU at J-PARC, which provides TOF neutron beams. Since the setting and coaxial alignment precision have a serious effect on the focusing ability in this experiment, these alignment methods have to be improved to obtain a high level of precision. However, the focused beam was successfully observed as a ring shape at the detector, and the MS mirror enabled us to perform an imaging test with a short exposure time of 10 s and a spatial resolution of $200\ \mu\text{m}$.

Acknowledgments

We are grateful to the staffs of the MLF at J-PARC for their help.

References

- [1] Nagano M, Yamaga F, Yamazaki D, Maruyama R, Hayashida H, Soyama K and Yamamura K 2012 *J. Phys. Conference Series* **340** 012016.
- [2] Nagano M, Yamaga F, Yamazaki D, Maruyama R, Hayashida H, Soyama K and Yamamura K 2012 *J. Phys. Conference Series* **340** 012034.
- [3] Liu D, Khaykovich B, Gubarev V. M, Robertson J. L, Crow L, Ramsey D. B and Moncton E. D 2013 *Nature Communications* **4** 2556.
- [4] Kardjilov N, Hilger M, Dawson M, Manke I, Banhart M, Strobl M and Boni P, 2010 *Journal of*

Applied Physics **108** 034905.

- [5] Kardjilov N, Manke I, Strobl M, Hilger A, Treimer W, Meissner M, Krist T and Banhart J 2008 *Nat. Phys.* **4** 399.
- [6] Shinohara T, Sakai K, Ohi M, Kai T, Harada M, Oikawa K, Maekawa F, Suzuki J, Oku T, Takata S, Aizawa K, Arai M and Kiyonagi Y 2011 *Nucl. Instrm. Meth. A* **651** 121.
- [7] Hayashida H, Yamazaki D, Ebisawa T, Maruyama R, Soyama K, Tasaki S, Hino M and Matsubayashi M 2011 *Nucl. Instrm. Meth. A* **634** S90.
- [8] Grunzweig C, Frei G, Lehmann E, Kuhne G and David C 2007 *Review of Scientific Instruments* **78** 053708.